Energy & Environmental Science

Accepted Manuscript

ROYAL SOCIETY OF CHEMISTRY

www.rsc.org/ees

Perovskite promoted iron oxide for hybrid water-splitting and syngas generation with exceptional conversion

Feng He, and Fanxing Li*

Department of Chemical and Biomolecular Engineering, North Carolina State University
911 Partners Way, Raleigh, NC 27695-7905, USA.
**Email: Fli5@ncsu.edu*

Abstract
We report a perovskite promoted iron oxide as a highly effective redox catalyst in a hybrid solar-redox scheme for methane partial oxidation and water-splitting. In contrast to previously reported ferrite materials, which typically exhibit 20% or lower steam to hydrogen conversion, $La_{0.8}Sr_{0.2}FeO_{3-\delta}$ (LSF) promoted Fe_3O_4 is capable of converting more than 67% steam with high redox stability. Both experiments and a defect model indicate that the synergistic effect of reduced LSF and metallic iron phases is attributable to the exceptional steam conversion. To further enhance such a synergistic effect, a layered reverse-flow reactor concept is proposed. Using this concept, over 77% steam to hydrogen conversion is achieved at 930 °C, which is 15% higher than the maximum conversion predicted by second law for unpromoted iron (oxides). When applied to the hybrid solar-redox scheme for liquid fuels and hydrogen co-generation, significant improvements in energy conversion efficiency can be achieved with reduced CO_2 emissions.

Besides being an important feedstock for petroleum and chemical industry, hydrogen is identified as an attractive, zero-emission fuel due to its high (weight-based) energy density.[1] At present, over 90% hydrogen is produced from fossil fuels, leading to notable greenhouse gas emissions from a life cycle standpoint. Unlike conventional reforming or gasification based approaches, water-splitting has the potential for hydrogen production with minimal environmental impacts. Extensive research has been conducted on H_2 generation using renewable resources.[2,3] Compared to photocatalytic water-splitting, thermochemical routes offer the potential to transform thermal energy to H_2 in a relatively simple yet effective manner. As an alternative to direct water thermolysis, which proceeds at extremely high temperatures (>3000 °C), two-step solar thermochemical water-splitting based on metal oxide reduction and oxidation (redox) cycles has emerged as a highly attractive approach.[4] Although a number of promising redox materials and schemes have been developed[4,5], the metal oxide reduction step in typical solar thermochemical water-splitting processes requires relatively high temperatures (> 1200 °C). In addition, steam conversion in the water-splitting step is often limited. An alternative redox-based approach for water-splitting is the steam–iron process.[6] In such a process, lattice oxygen in iron oxides is first removed by syngas, producing wüstite and/or metallic iron. The reduced ferrites are then used for water-splitting and hydrogen generation. A number of (supported) iron oxides[6], including Fe_3O_4-CeO_2-ZrO_2[7], Fe_3O_4-Al_2O_3[8,9], Fe_3O_4-$MgAl_2O_4$[10] and Fe_3O_4-$Ce_{0.5}Zr_{0.5}O_2$[11], have been investigated for steam-iron applications. The reported steam to hydrogen conversion is generally less than 20%. This, coupled with incomplete syngas

conversion during the iron oxide reduction step, limits the process efficiency. We reported a hybrid solar-redox scheme for liquid fuel and hydrogen co-production from methane and solar energy.[12] Using a perovskite-supported iron oxide, high process efficiency and near zero CO_2 emissions for hydrogen generation are shown to be feasible. A key factor for the significantly improved efficiency resides in the high steam to hydrogen conversion for water-splitting.

Low steam conversion in the water-splitting step will exert inevitable energy penalty on the process, since the second law dictates that latent heat in the steam-H_2 product mixture cannot be fully recuperated. A second law analysis (see ESI) indicates >3 kJ of exergy loss for every additional mole of unconverted steam. In practice, steam to hydrogen conversion for metallic iron and iron oxides is thermodynamically limited. For instance, at 930 °C, a maximum steam to hydrogen conversion of 62.3% is calculated by thermodynamic equilibrium of the FeO_x-H_2O-H_2 ternary system (see ESI). Many of the iron containing redox materials exhibit even lower affinity to oxygen, leading to lower equilibrium constants for the water-splitting reaction (Reaction 1). The present article reports a highly effective, ferrite-based redox material for combined methane partial oxidation and water-splitting. Using perovskite-promoted iron oxide coupled with a layered reverse-flow reactor concept, over 77% steam to hydrogen conversion is achieved at 930 °C. The exceptional conversion, which is 15% higher than the maximum conversion predicted by the second law for iron (oxides), is achieved through synergistic effects between iron oxide and its perovskite support as well as a novel, layered reverse-flow reactor concept.

$$MeO_{x-1} + H_2O \leftrightarrow MeO_x + H_2 \qquad \text{Reaction 1}$$

To validate their high efficacy for water-splitting, iron oxides with 25% and 40% $La_{0.8}Sr_{0.2}FeO_{3-\delta}$ (LSF) support are prepared and tested in a fixed-bed reactor. The primary role of LSF support is to provide ionic and electronic conduction pathways for effective removal and replenishment of active lattice oxygen in iron oxides. Such an effect has been confirmed through our recent studies.[12–15] A reduced iron phase is first created by contacting the redox material with hydrogen or CO. H_2 is used as reducing gas to rule out coke formation and its subsequent contribution towards H_2 generation through steam-carbon reaction. When re-oxidized, steam to H_2 conversion of these perovskite-supported redox materials (64±0.7% and 67±1.3%) as shown in Figure 1 are consistently higher than those predicted by the FeO_x-H_2O-H_2 equilibrium (62.3%) at 930 °C. Excellent stability is also achieved over multiple redox cycles (see ESI). Similar steam conversions are observed for redox materials reduced with CO. The exceptional steam conversion with LSF-supported iron oxide, which is higher than the nominal thermodynamic limit of 62.3%, is certainly not unphysical. Rather, it can be explained by the high oxygen affinity of LSF precursors as well as the oxygen vacancies in reduced LSF.

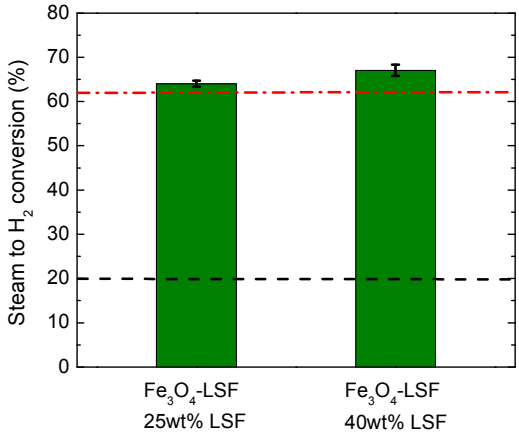

Figure 1: Average steam conversion (%) of Fe_3O_4-LSF in the oxidation step at 930 °C (regenerated to an average composition of $FeO_{0.5}$). Error bars indicate 95% confidence interval for steam conversion form multi-cycle experiments (see ESI). Red dash-dotted line shows the maximum steam conversion for FeO_x-H_2O-H_2 ternary system based on thermodynamic equilibrium. Black dashed line shows the highest literature-reported steam conversion.[6–11]

In order to reveal the contribution of LSF to the overall water-splitting reaction, steam oxidation of reduced LSF-Fe_2O_3 is conducted in a thermal gravimetric analyzer (TGA). A H_2-steam mixture with decreasing H_2 concentrations is introduced into the TGA, and the sample weight change is recorded. Weight gain of the sample under a specific H_2 concentration, defined as $F_{H2}(F_{H2}+F_{H2O})^{-1}$, indicates that the sample is capable of achieving the corresponding or higher steam to H_2 conversion. In Figure 2A, four regions are found under varying H_2 concentrations. The corresponding phases are analyzed by X-ray powder diffraction (XRD) (Figure 2B). The reduced redox material is primarily composed of a composite of Fe, La_2O_3, and a very small amount of $LaSrFeO_{4-\delta}$. These reduced metallic iron and oxide species are stable under 100% H_2 (Region I). However, they are easily oxidizable even in the presence 95% H_2 balanced steam ($P_{O2}=5\times10^{-19}$ atm at 930 °C). Such a high affinity to oxygen is not observed in a pure Fe-O system, as iron is only oxidized to wüstite at $P_{O2} = 6\times10^{-17}$ or higher (equivalent to 62.3% steam conversion). The main driving force for the exceptional steam conversion, as evidenced by XRD spectra of the partially oxidized sample in Region II, is the solid state reaction among iron, La_2O_3, and SrO in the presence of water as well as water-splitting reaction of defected LSF. Such reactions can be generalized as:

$$La_{0.8}Sr_{0.2}FeO_{3-\delta} + (\delta' - \delta)\, H_2O \leftrightarrows La_{0.8}Sr_{0.2}FeO_{3-\delta'} + (\delta' - \delta)\, H_2 \qquad \text{Reaction 2}$$

where $0 \le \delta < \delta' \le 1.6$. The specific reaction involved in Region II is:

$$0.4La_2O_3 + 0.2SrO + Fe + (1.6 - \delta)\, H_2O \leftrightarrows La_{0.8}Sr_{0.2}FeO_{3-\delta} + H_2 \qquad \text{Reaction 3}$$

Reaction 3 can be considered as a special case of Reaction 2, under which the oxygen defect concentration is too large to maintain a stable perovskite structure. The contribution of Reactions 2 and 3 to overall water-splitting reaction can be determined based on defect formation energies in LSF perovskites, which can accommodate significant oxygen non-stoichiometry resulting from acceptor (Sr) doping in its A-site cations and the variable valence states of its B-site (Fe)

cations.[16] Using the defect model proposed by Mizusaki and Murugan et al[17–19], the relationship between oxygen vacancy (δ) and oxygen partial pressure is determined by:

$$\frac{\delta^{\frac{1}{2}}(2\delta - x + 1)}{(3-\delta)^{\frac{1}{2}}(2\delta - x)} p_{o_2}^{\frac{1}{4}} = \frac{K_{Fe}}{K_{Ox}} \frac{(1+x-2\delta)(3-\delta)^{\frac{1}{2}}}{\delta^{\frac{1}{2}}(2\delta - x)} \frac{1}{p_{o_2}^{\frac{1}{4}}} - \frac{1}{K_{Ox}^{\frac{1}{2}}} \qquad \text{Equation 1}$$

where $x = 0.2$ for $La_{0.8}Sr_{0.2}FeO_{3-\delta}$. Since the above model is suited for defected perovskites with very high steam conversions, it can accurately estimate steam conversions in both Reaction 2 and 3. As shown in Figure 2A, the model predictions (see ESI for details) are in good agreement with TGA results. The slight over-prediction in Region II and III is partly due to incomplete reduction of the sample prior to steam oxidation, as confirmed by XRD in Figure 2B.

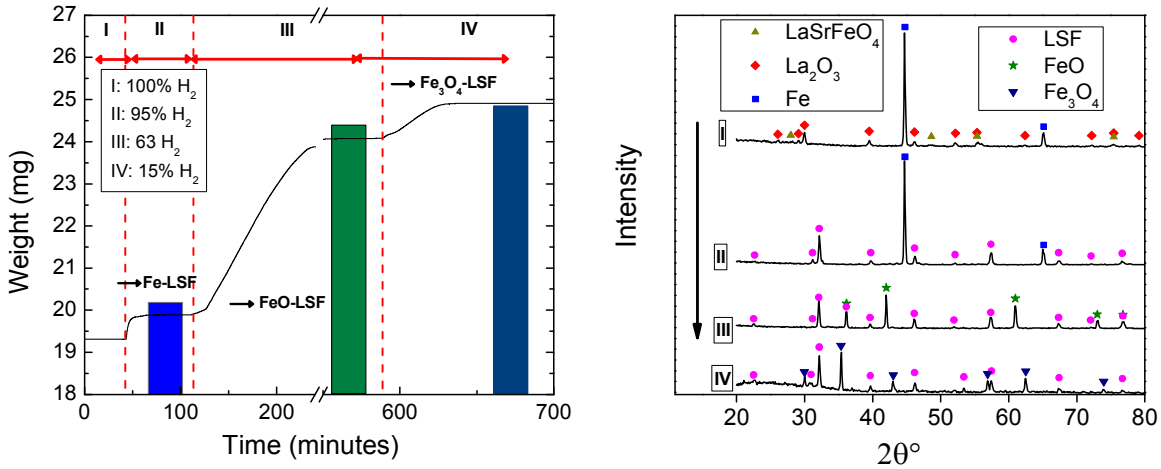

(A) (B)

Figure 2: (A) TGA profile of the reduced Fe_3O_4-LSF particle oxidized by steam and hydrogen mixture at 930°C. (I) in the presence of pure H_2; (II) oxidized by 95% H_2 (balance steam,N_2-free basis); (II) oxidized by 63% H_2; (IV) oxidized by 15% H_2. (B) XRD results of the particles when weight is stabilized in regimes (I), (II), (III) and (IV).

In the subsequent oxidation step in Region III, the main oxygen acceptor for water-splitting is metallic iron, forming wüstite. Oxygen vacancies in the LSF phase also contribute to a small fraction of the oxygen uptake. The corresponding steam to H_2 conversion in such a step is shown to be around 63%, which is in-line with equilibrium steam conversion between Fe to FeO (62.3%). As confirmed via TGA, iron (oxide), through phase transition from iron to wüstite, is responsible for 85.8% of the hydrogen generated from water-splitting with the LSF phase contributing the remaining 14.2%. The contribution from the LSF phase, albeit small, is essential for steam conversion (Figure 3A). Based on the defect model, theoretical steam conversion for 25 wt% LSF promoted iron oxide is predicted to be 65.7% assuming iron and LSF phases act independently for water-splitting (additive effect). Besides the abovementioned additive effect, which is appropriate to describe composite LSF-iron oxide redox catalysts in a conventional fixed bed, one can also envision a scenario under which steam reacts with reduced iron (oxide) and LSF in a sequential manner. Such a configuration puts steam in sequential contact with two

redox materials with increasing oxygen affinity (or water-splitting efficacy). As a result, the overall thermodynamic driving force for water-splitting is maximized. As illustrated in Figure 3B, further improvement in steam conversion can be anticipated under the sequential case.

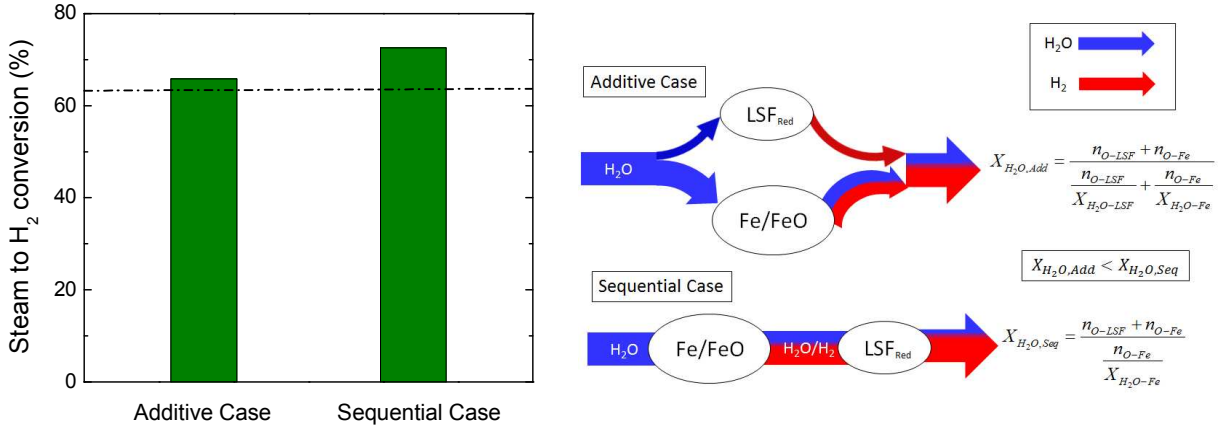

(A) (B)

Figure 3: (A) Equilibrium steam conversion calculated based on an additive effect and sequential effect for iron oxide promoted with 25wt% LSF at 930 °C; (B) Schematic illustration of the additive and sequential cases. $n_{O\text{-}Fe}$ and $n_{O\text{-}LSF}$ represent the oxygen uptake by reduced iron oxide and LSF during water-splitting. $X_{O\text{-}Fe}$ and $X_{O\text{-}LSF}$ are equilibrium steam conversions for reduced iron oxide and LSF. $X_{H2O,Add}$ and $X_{H2O,Seq}$ refer to overall steam conversion in additive case and sequential case (equations shown are generally applicable to redox catalysts with <50 wt% LSF).

In order to achieve the perceived advantage of the sequential reaction scheme, a layered reverse-flow reactor design using Fe_3O_4-LSF is proposed for combined syngas generation and water-splitting. As illustrated in Figure 4, the reactor is composed of two layers. The bottom layer is iron (oxide) rich, whereas the top layer is primarily composed of LSF. A small amount of LSF at the bottom layer is necessary to prevent iron oxide sintering and deactivation. During the syngas generation stage, methane is introduced from the top of the reactor, producing syngas while removing the active lattice oxygen from both LSF and iron oxide-LSF layers. Since LSF has higher resistance towards coke formation,[15] injecting methane from the LSF end would be advantageous. Upon completion of the reduction reaction, steam is introduced from the bottom of the reactor to react with the reduced iron oxide-LSF layer and then the LSF layer. Such an arrangement maximizes the thermodynamic driving force for water-splitting while taking advantage of the unique properties of LSF for methane partial oxidation. As a result, high syngas yield and exceptional steam conversion can be achieved. The concept illustrated in Figure 4 can be extended to general cases where concentration gradients of LSF and iron oxide are created along axial position of the fixed bed reactor.

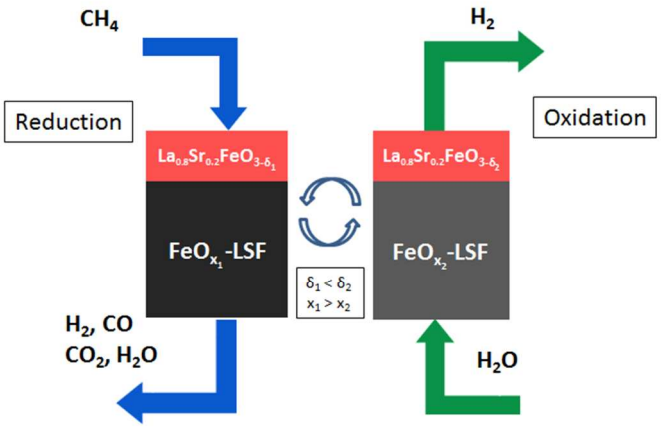

Figure 4: Schematic of the proposed layered reverse-flow redox process with exceptional steam conversion and syngas yield.

Fixed bed testing is performed to validate the layered reverse-flow concept. The reactor is comprised of an LSF layer added on top of an LSF-iron oxide layer. Overall, the reactor is comprised of 55% iron oxide with a balance of LSF. Key results of the redox reactions are summarized in Table 1. 99% methane conversion and 62% (±3%) syngas yield was achieved in the reduction step. In the oxidation step, steam conversion in excess of 77% was achieved. A comparison of steam conversion is illustrated in Figure 5. Using the layered reverse-flow concept, steam conversion was increased by over 10% when compared to a regular fixed bed. Such a conversion is also 15% higher than thermodynamically predicted conversion for pure iron oxides, which is the main contributor to water-splitting. An ASPEN Plus® model is used to simulate the performance of the layered reverse-flow concept in the hybrid solar-redox scheme.[12,20] Based on the experimental data, the overall process efficiency is determined to be 63.1% (HHV) or 15.1% higher than a case with 20% steam conversion (maximum steam conversion reported in literature). It is noted that steam conversion in excess of 77% is also feasible by adjusting the relative amounts of LSF and iron oxide in the reactor. Figure 6 illustrates the relationships among La/Sr usage, H_2 generation capacity, and steam conversion. As can be seen, increase in La/Sr usage increases steam conversion. In the meantime, H_2 generation capacity of the redox caco

Table 1: Summary of the redox reactions performance

Syngas yield moles (mole of methane)$^{-1}$	1.78
H_2 yield moles (mole of methane)$^{-1}$	1.93
Methane conversion	99%
Steam conversion	77.2%
Hydrogen purity	98.5%
ASPEN simulated process efficiency	63.1% (HHV)

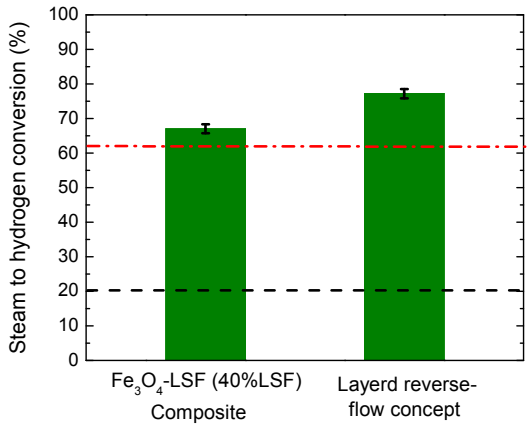

Figure 5: Steam to hydrogen conversion in the oxidation step after CH_4 reduction at 930 °C. Red dash-dotted line displays thermodynamically predicted maximum steam conversion for FeO_x-H_2O-H_2 ternary system. Black dashed line shows the highest literature reported steam conversion.[6–11]

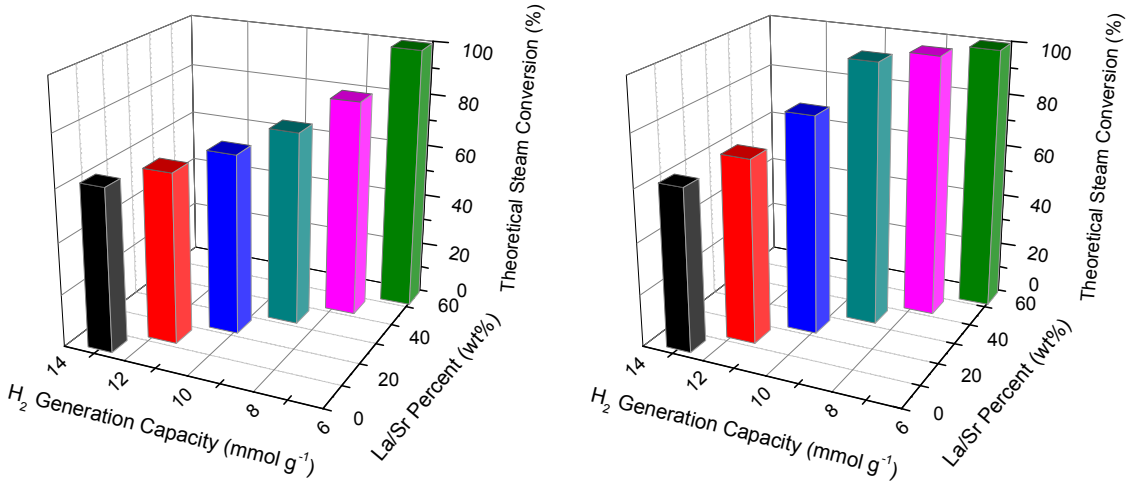

(A) (B)

Figure 6: Theoretical conversion as a function of La/Sr content and H_2 generation capacity in (A) regular fixed bed; (B) layered reverse-flow reactor.

In summary, LSF-promoted iron oxide is demonstrated to be an exceptional redox material in a hybrid redox scheme for methane partial oxidation and water-splitting. Coupled with a novel layered reverse-flow reactor concept, the redox material is shown to be capable of converting over 77.2% steam into hydrogen. Such a conversion not only triples the performance of existing thermochemical based water-splitting processes, but also significantly exceeds the theoretical water-splitting efficiency for unpromoted iron oxides. When applied to the hybrid solar-redox scheme for liquid fuel and hydrogen co-generation, the process efficiency can increase by 15.1% (HHV) and CO_2 emission for H_2 product is reduced by up to 60%.

Acknowledgments
This work is supported by the U.S. National Science Foundation (CBET-1254351) and the Army Research Office DURIP program (61607-CH-RIP).

Keywords: hydrogen • iron oxide • methane • perovskite • water splitting

References:

1 J. M. Ogden, *Annu. Rev. Energy Environ.*, 1999, **24**, 227–279.
2 M. G. Walter, E. L. Warren, J. R. McKone, S. W. Boettcher, Q. Mi, E. A. Santori and N. S. Lewis, *Chem. Rev.*, 2010, **110**, 6446–6473.
3 J. Luo, J.-H. Im, M. T. Mayer, M. Schreier, M. K. Nazeeruddin, N.-G. Park, S. D. Tilley, H. J. Fan and M. Grätzel, *Science*, 2014, **345**, 1593–1596.
4 W. C. Chueh, C. Falter, M. Abbott, D. Scipio, P. Furler, S. M. Haile and A. Steinfeld, *Science*, 2010, **330**, 1797–1801.
5 C. L. Muhich, B. W. Evanko, K. C. Weston, P. Lichty, X. Liang, J. Martinek, C. B. Musgrave and A. W. Weimer, *Science*, 2013, **341**, 540–542.
6 K. S. Go, S. R. Son, S. D. Kim, K. S. Kang and C. S. Park, *Int. J. Hydrog. Energy*, 2009, **34**, 1301–1309.
7 D. Yamaguchi, L. Tang, L. Wong, N. Burke, D. Trimm, K. Nguyen and K. Chiang, *Int. J. Hydrog. Energy*, 2011, **36**, 6646–6656.
8 P. R. Kidambi, J. P. E. Cleeton, S. A. Scott, J. S. Dennis and C. D. Bohn, *Energy Fuels*, 2012, **26**, 603–617.
9 A. M. Kierzkowska, C. D. Bohn, S. A. Scott, J. P. Cleeton, J. S. Dennis and C. R. Müller, *Ind. Eng. Chem. Res.*, 2010, **49**, 5383–5391.
10 M. Rydén and M. Arjmand, *Int. J. Hydrog. Energy*, 2012, **37**, 4843–4854.
11 V. Galvita, T. Hempel, H. Lorenz, L. K. Rihko-Struckmann and K. Sundmacher, *Ind. Eng. Chem. Res.*, 2008, **47**, 303–310.
12 F. He, J. Trainham, G. Parsons, J. S. Newman and F. Li, *Energy Environ. Sci.*, 2014, **7**, 2033–2042.
13 N. L. Galinsky, Y. Huang, A. Shafiefarhood and F. Li, *ACS Sustain. Chem. Eng.*, 2013, **1**, 364–373.
14 A. Shafiefarhood, N. Galinsky, Y. Huang, Y. Chen and F. Li, *ChemCatChem*, 2014, **6**, 790–799.
15 L. M. Neal, A. Shafiefarhood and F. Li, *ACS Catal.*, 2014, **10**, 3560–3569.
16 M. A. Peña and J. L. G. Fierro, *Chem. Rev.*, 2001, **101**, 1981–2018.
17 J. Mizusaki, T. Sasamoto, W. R. Cannon and H. K. Bowen, *J. Am. Ceram. Soc.*, 1983, **66**, 247–252.
18 J. Mizusaki, M. Yoshihiro, S. Yamauchi and K. Fueki, *J. Solid State Chem.*, 1985, **58**, 257–266.
19 A. Murugan, A. Thursfield and I. S. Metcalfe, *Energy Environ. Sci.*, 2011, **4**, 4639–4649.
20 F. He and F. Li, *Int. J. Hydrog. Energy*, 2014, **39**, 18092–18102.

Under a cyclic redox mode, a perovskite promoted iron oxide exhibited 77% steam-to-hydrogen conversion in a layered reverse-flow reactor.